# Transmission risk of SARS-CoV-2 in the watershed triggered by domestic wastewater discharge

Zhenyu Wang [c,1], Wenyu Yang [c,1], Pei Hua [a,b,*], Jin Zhang [d], Peter Krebs [c]

[a] SCNU Environmental Research Institute, Guangdong Provincial Key Laboratory of Chemical Pollution and Environmental Safety & MOE Key Laboratory of Theoretical Chemistry of Environment, South China Normal University, China
[b] School of Environment, South China Normal University, University Town, Guangzhou, China
[c] Institute of Urban and Industrial Water Management, Technische Universität Dresden, 01062 Dresden, Germany
[d] Department of Ecology and Institute of Hydrobiology, Jinan University, 510632 Guangzhou, China

## HIGHLIGHTS

- Description of the SARS-CoV-2 transmission in a large watershed
- Evaluation of the multifactorial impact on virus transmission in surface water
- Improvement of the infection probability estimation of SARS-CoV-2 from surface water by using protected RNA genomes

## GRAPHICAL ABSTRACT
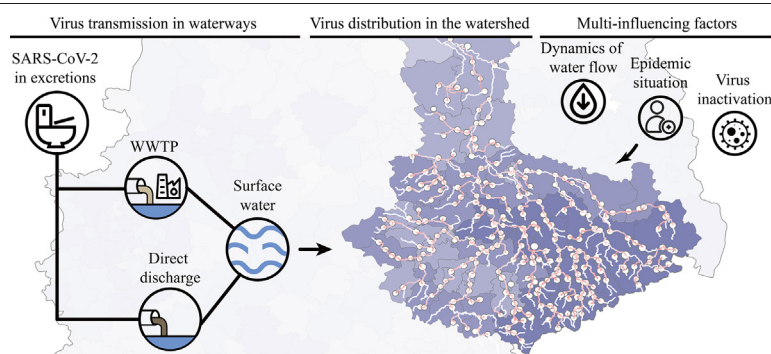


## ARTICLE INFO

## ABSTRACT

The outbreak of COVID-19, caused by severe acute respiratory syndrome coronavirus 2 (SARS-CoV-2), has already become an unprecedented global pandemic. However, the transmission of SARS-CoV-2, especially the protected SARS-CoV-2 RNA (pRNA) with infectious particles in waterways, is still largely unexplored. In this study, we developed a model to estimate SARS-CoV-2 transmission from the risk source in the excretion of patients to the final exposure in surface water. The model simulated the spatial and temporal distribution of the viral pRNA concentrations in the surface water of the Elbe watershed from March 2020 to January 2021. The results show that the WWTPs with the maximum capacity of >10,000 population equivalents were responsible for 95% of the viral load discharged into the surface water. We estimated the pRNA concentrations in surface water to be $1.33 \times 10^{-2}$ copies·L$^{-1}$ on average in the watershed based on the model simulation on viral transmission. It had considerable variations in spatial and temporal scales, which are dominantly controlled by epidemic situations and virus transport with decay in water, respectively. A quantitative microbial risk assessment was conducted to estimate the viral infection probability from surface water ingestion with consideration of the influence of toilet usage frequency and gender/age population groups. All the infection probabilities in the study period were lower than the reference risk levels of $10^{-4}$ and $10^{-5}$. The individuals aged 15–34 years had the highest infection probability of $4.86 \times 10^{-9}$ on average from surface water ingestion during swimming activities. The data provided herein suggest that the low pRNA concentrations and infection probability reflected that the waterways were unlikely to be a significant transmission route for SARS-CoV-2.

© 2021 Elsevier B.V. All rights reserved.

* Corresponding author at: School of Environment, South China Normal University, University Town, Guangzhou, China.
E-mail address: pei.hua@m.scnu.edu.cn (P. Hua).
[1] These authors contributed equally to this work.

# 1. Introduction

The ongoing coronavirus disease 2019 (COVID-19) pandemic caused by severe acute respiratory syndrome coronavirus 2 (SARS-CoV-2) has resulted in severe impacts on public health and the worldwide economy (Kissler et al., 2020; Kraemer et al., 2020; Mawani and Li, 2020). The rapid transmission of SARS-CoV-2 has developed into an unprecedented global challenge. As of March 2021, there had been over 122,000,000 confirmed cases of COVID-19, including over 2,650,000 deaths globally (WHO, 2021). It was forecasted that there would be an approximate loss of 4.2% in global annual gross domestic product growth within a year (OECD, 2021a). Up to 1st April 2021, the European Economic Area still had a 14-day notification rate of 490 new cases per 100,000 inhabitants, and Germany's 7-day incidence was 134 per 100,000, higher than the critical rate of 100 per 100,000 (RKI, 2021). Therefore, controlling this rapid worldwide transmission needs global cooperation and a better understanding of the viral transmission pathway is crucial for the effective implementation of anti-epidemic measures.

In this regard, the transmission of SARS-CoV-2 through respiratory droplets from infected people, aerosols, and fomites has been intensively reported (Asadi et al., 2020; Chan et al., 2020; Chia et al., 2020). By contrast, the other transmission pathways of SARS-CoV-2 are still largely unexplored. The investigation of a SARS-CoV-1 outbreak from an apartment building in Hong Kong in 2003 highlighted the role of the sewage system in the transmission risk of SARS-CoVs in waterways (McKinney et al., 2006). Specifically, SARS-CoV infection may occur through consumption of contaminated water droplets or respiration of aerosols created from toilet flushing (Gormley et al., 2020), defective plumbing systems (Yu et al., 2014), or uncovered aerobic wastewater treatment facilities (Gholipour et al., 2021). As the viral RNA of SARS-CoV-2 was also found in excretions (stool and urine) of symptomatic and asymptomatic patients (Guan et al., 2020; Pan et al., 2020) as well as wastewater (Ahmed et al., 2020; Haramoto et al., 2020), the potential infection risk of SARS-CoV-2 from waterways during the pandemic has been of increasing concern.

The SARS-CoV-2 load has been reported in natural receiving water in low sanitation countries (Guerrero-Latorre et al., 2020). However, the transmission of SARS-CoV-2 in waterways is unclear due to the complicated multifactorial impacts of the epidemic situation, discharges of wastewater treatment plants (WWTPs), dynamics of water flows, and lack of understanding of SARS-CoV-2 persistence and decay in natural waterways outside the laboratory environment (Kumar et al., 2021; Mohapatra et al., 2021; Paul et al., 2021). Several studies have

conducted a risk analysis of SARS-CoV-2 in wastewater and wastewater-impacted surface water through quantitative microbial risk assessment (QMRA) (Dada and Gyawali, 2021; Yang et al., 2020; Zaneti et al., 2021). However, most of the studies did not account for the total RNA to infectious virus ratios in waterways, and it could highly overestimate the actual infection risk (Ahmed et al., 2021). In addition, the spatiotemporal distribution of SARS-CoV-2 transported in the surface water of a watershed during the pandemic has not been evaluated. There is still uncertainty surrounding the actual probability of wastewater-dependent SARS-CoV-2 transmission risk in a watershed with multiple WWTPs. It has been reported that the concentration of SARS-CoV-2 genomes, protected by viral proteins and surrounded by a cell-derived envelope in infectious particles (or called protected RNAs, pRNA), was closer to the infectious virus concentration rather than the total RNA (vRNA) concentration in wastewater detected by RT-qPCR (Wurtzer et al., 2021). Therefore, it is essential to redevelop a model addressing SARS-CoV-2 pRNA transmission from excretions and wastewater to surface water in a watershed.

Hence, in this study, we developed a descriptive model of virus transmission in a large watershed and a quantitative microbial risk assessment to describe the relationship between virus intake and incidence. The focuses of this study were to (1) credibly estimate the spatiotemporal distribution of SARS-CoV-2 pRNA concentration in surface waters, (2) investigate the most influential factors of SARS-CoV-2 transmission in surface water with the consideration of model uncertainty and sensitivity, and (3) assess the infection probability from the contaminated surface water. The methods and findings provided herein are expected to assist the controlling policies and provide an additional reference to mitigate the SARS-CoV-2 transmission in the waterways.

# 2. Materials and methods

## 2.1. Study area and epidemic situation

We estimated SARS-CoV-2 transmission in the Elbe watershed in Germany during the pandemic from 25th Mar 2020 to 10th Jan 2021. The Elbe watershed is composed of the Elbe main channel, Saale watershed, Mulde watershed, and Schwarze Elster watershed (Fig. 1a). The study areas in Saxony, Thuringia, Saxony-Anhalt, and Brandenburg account for 41.2%, 19.2%, 36.8%, and 2.9% of the rivers and streams, respectively, and 47.8%, 21.1%, 27.5%, and 3.6% of the population, respectively. The model used epidemic data from 46 districts, wastewater data from 280 WWTPs, and surface water flow data from 186 discharge
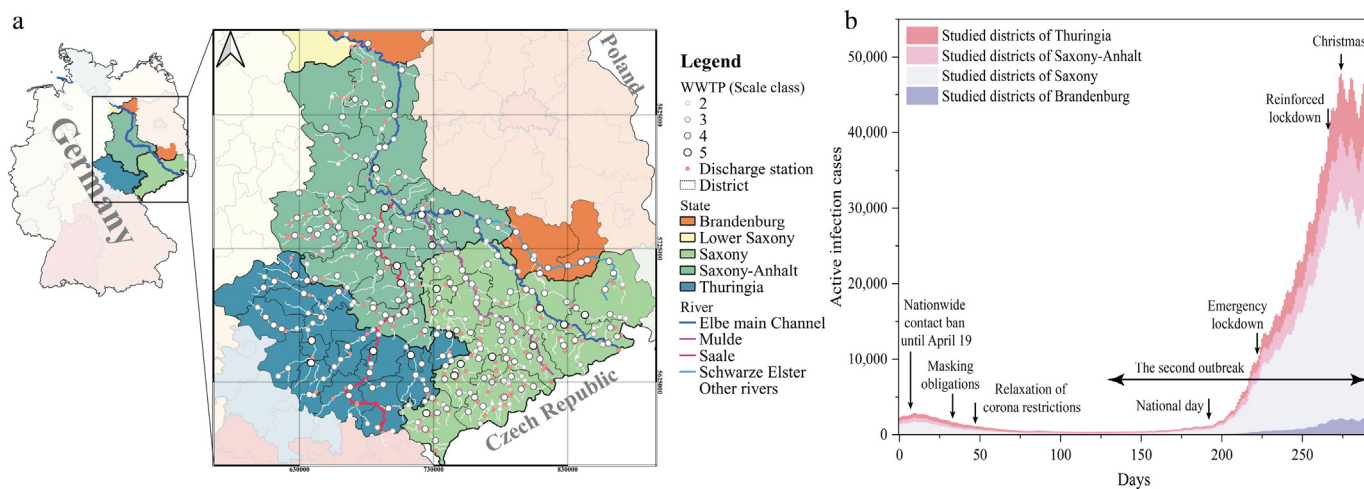


**Fig. 1.** a). Map of the study Elbe watershed containing 186 rivers and streams, 280 wastewater treatment plants, and 186 discharge monitoring sites in the study. The coordinate reference system of the map is ETRS89/UTM zone 32N. b) The time series of active infection cases in the study districts of four states are shown as stacked columns. The government interventions are noted.

monitoring sites to estimate the transmission of SARS-CoV-2 from the source in the excretion of patients to the final exposure in surface water.

The study area experienced two waves of COVID-19, namely the first wave in March–May 2020 and the second wave in August–January 2020 (Fig. 1b). The number of active infection cases in the study period ranged from 347 to 47,781. Saxony state accounted for the highest proportion of active infection cases (25.2–68.1%) in the study region, followed by Thuringia (24.9–39.8%), and Saxony-Anhalt (21.7–34.6%). The district-level distribution of active infection cases and cases in 100,000 inhabitants are shown in Fig. 2 and Figs. S1–3, respectively.

### 2.2. SARS-CoV-2 concentrations in waterways

The SARS-CoV-2 concentrations in waterways were calculated by considering the daily toilet usage, regional epidemic situation, SARS-CoV-2 removal in WWTPs, and discharge-dependent transmission in surface water with dilution and decay. The discharge-dependent SARS-CoV-2 concentrations in surface water were calculated as follows (Yang et al., 2020):

$$\mu = \frac{d_{eff} \cdot \delta}{Q} \cdot c \tag{1}$$

where $\mu$ is the virus concentration (copies·L$^{-1}$); $d_{eff}$ is the daily virus amount in the WWTP effluent (copies); $Q$ is the surface-water flow rate, which is the sum of river/stream flow rates and WWTP effluent flow rates (m$^3$/d), and the WWTP effluent flow rates in units of m$^3$/d were yielded by averaging annual effluent volume (m$^3$/year) over a year; $c$

is the unit conversion factor; and $\delta$ is the viral inactivation rate or decay rate described as first-order distance-dependent decay kinetics shown as Eq. (2) (Fauvel et al., 2017).

$$\delta = e^{-\gamma L} \tag{2}$$

where the first-order inactivation parameter $\gamma$ is parameterized by a lognormal distribution, and $L$ is the distance (m).

The WWTP status and regional epidemic situation exert significant influences on the variable $d_{eff}$ (Eqs. (3)–(5)).

$$d_{eff} = r \cdot n \cdot N \cdot \left( (1 - \theta_v) + \frac{1 - \lambda_c}{\lambda_c} \right) \tag{3}$$

$$N = \beta \cdot P \tag{4}$$

$$P = PE \cdot \lambda_p \tag{5}$$

where $r$ is the protected RNA to total RNA ratio (pRNA/vRNA), which was determined based on a previous study (Wurtzer et al., 2021); $n$ is the total viral RNA amount discharged into sewage per person per day (copies·person$^{-1}$·day$^{-1}$); $\theta_v$ is the virus removal efficiency of WWTPs; $\lambda_c$ is the population connection rate to WWTPs or the percentage of treated wastewater; $N$ is the COVID-19 infection cases connected to WWTPs, which is proportional to population connected to WWTPs, $P$ and the regional infection rate, $\beta$; $P$ is estimated by the maximum structural capacity of a WWTP in population equivalents (PE) and the domestic wastewater proportion $\lambda_p$. Since the temporal change of the regional population can cause the design value of $P$ in
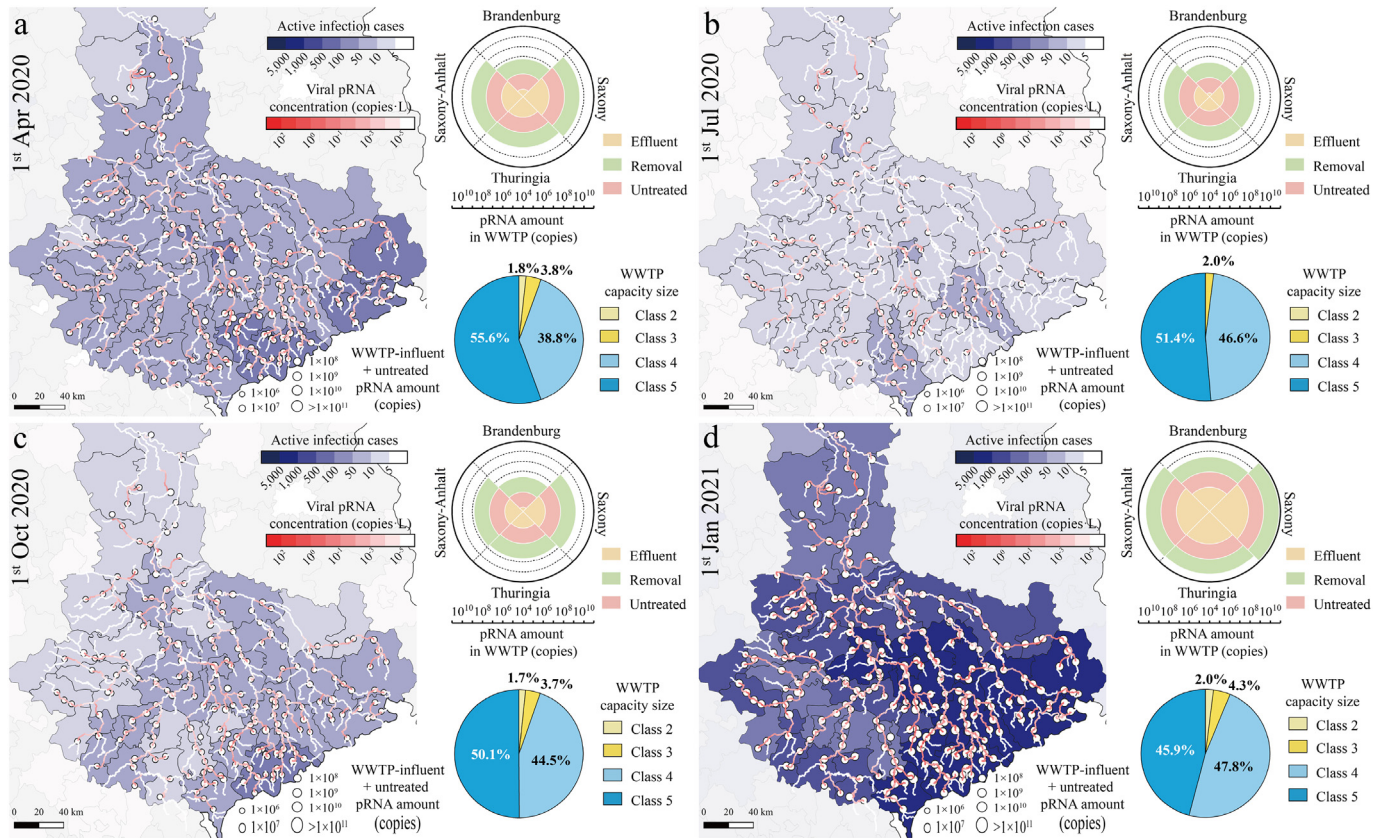


Fig. 2. The geographic distribution of the district-level of COVID-19 epidemic situation, the estimated median SARS-CoV-2 pRNA amount discharged from WWTPs, and the estimated median pRNA concentrations along the rivers of the study Elbe in a) Apr 2020, b) June 2020, c) October 2020 and d) January 2021. It included the COVID-19 active infection cases (blue color shading), pRNA concentrations in surface water in copies·L$^{-1}$ (red color shading), and the sum of WWTP-influent and untreated pRNA amount in copies (white round label). Charts on the left show the sum of treated, removed, and discharged pRNA amount (copies) from state-level WWTPs (windrose chart) and the percentage of the discharged pRNA amount (copies) from WWTPs of 2–5 capacity sizes (pie chart).

the region to exceed the current WWTP-connected population, $P$ in part of the districts is normalized by scaling the $\sum P$ to $\lambda_c$ population in the district.

Moreover, $n$ is calculated as follows (Yang et al., 2020):

$$n = \varphi_u \cdot v_u \cdot n_u + \varphi_s \cdot m_s \cdot n_s \tag{6}$$

where $\varphi$, $v/m$, and $n$ are the toilet usage frequency constant controlled by the people's reaction to the government interventions, daily volume or mass of a patient's excretions (mL for urine; g for faeces), and the genome vRNA concentration in a patient's excretions (copies·mL$^{-1}$ for urine; copies·g$^{-1}$ for faeces), respectively. Subscripts $s$ and $n$ are stool and urine, respectively.

The values for all parameters are parameterized as shown in Table 1 based on the published scientific literature (Tables S2–6). The unit of copies·mL$^{-1}$ for the genome vRNA concentration in faeces reported in the literature was converted to copies·g$^{-1}$ by using a density of wet human faeces of 1.075 g·mL$^{-1}$ (Penn et al., 2018). The best-fit distributions of parameters were selected based on the Kolmogorov–Smirnov analysis ($p < 0.05$).

### 2.3. QMRA model

The infection probability of SARS-CoV-2 from surface water ingestion was estimated by using the estimated genome pRNA concentrations in the surface water and the dose–response relationship alongside QMRA models (Haas et al., 2014). The probability of infection was characterized by a modified exponential dose-response function, as given in Eq. (7) (Watanabe et al., 2010; Zhang and Wang, 2020b).

$$P_{inf}(d) = \left(1 - e^{-kd_{ex}}\right) \cdot \alpha \tag{7}$$

where $k$ is the dose-response parameter; $d_{ex}$ is the exposure dose of ingested pathogens in an event in a day (copies·day$^{-1}$), and $\alpha$ is the infection rate constant for the specific age and gender groups according to the German COVID-19 infection data (Table S4). $k$ is modelled by using a log-normal distribution, and $d_{ex}$ is calculated from Eq. (8) according to the previous study (Yang et al., 2020).

$$d_{ex} = \mu \cdot m \tag{8}$$

where $m$ is the water exposure dose per person in an event in a day (mL·person$^{-1}$·day$^{-1}$). $m$ is described by the gamma distribution for the swimming activity. The values of the model parameters are shown in Table 1.

The estimated infection probabilities were compared with the reference risk levels suggested by the US EPA (Gholipour et al., 2021) and WHO (Mara et al., 2007). The reference risk levels were in units of person$^{-1}$·year$^{-1}$, and they were converted into person$^{-1}$·day$^{-1}$ based on Eq. (9) (Moazeni et al., 2017):

$$P_{inf(D)} = 1 - \sqrt[n]{\left(1 - P_{inf(A)}\right)} \tag{9}$$

where n is the exposure frequency per year, which was 7 times per year in the study (Schets et al., 2011).

### 2.4. Uncertainty and sensitivity analysis

Since there is a large variability for most of the parameters used in the model, the results were estimated by a Latin-hypercube-sampling-based Monte Carlo simulation. The Monte Carlo simulation drew 10,000 trials to create a distribution of infection probabilities. The uncertainty of the results was described as a 95% confidence interval. The estimated median results were used to make a conservative estimation of the viral concentrations in the surface water and the infection probability.

The sensitivity of the estimated SARS-CoV-2 concentrations was analysed utilizing Sobol's method and rank correlation. Sobol's method calculated the total Sobol's sensitivity index $S_{Ti}$ to describe the ratio between the variance derived from the $i^{th}$ parameter and interactions of all the other parameters (Sobol, 2001; Vezzaro and Mikkelsen, 2012) (Eq. (10)).

$$S_{Ti} = \frac{E_{X_i}\left(Var_{X_i}\left(Y|X_{\bar{i}}\right)\right)}{Var(Y)} \tag{10}$$

The rank correlation was determined by utilizing the Spearman rank correlation $\rho$ between each model parameter and the estimated infection probability (Bivins et al., 2017). Both methods were conducted by Latin-hypercube sampling. The numerical results of the sensitivity analysis are summarized in Tables S7–8. The uncertainty and sensitivity analysis was conducted using Python 3.7.

### 2.5. Scenario analysis

The risk was classified into the scenarios of toilet usage frequency caused by the patients' psychological stress during lockdown (normal and increasing usage frequency; N and I), the age groups (5–14, 15–34, 5–59, and 60–79 years old) and the gender groups (male and female; M and F) by varying the model parameters. The detailed statistical analysis of toilet usage frequency is presented in Supplementary material S1. The scenario-based variation in parameter values is shown in Table 1.

### 2.6. Data handling and statistical analysis

The river discharge data were provided by the State Office for the Environment, Agriculture, and Geology of Saxony (LfULG) and Flood Forecasting Centre of Saxony-Anhalt (HVZ). The data of the annual effluent volume, the maximum structural capacities, the wastewater treatment approaches and locations of WWTPs were from the European Municipal Waste Directive (EKR, 2016). The epidemic data of cumulated infection cases and death in German districts were provided by the Robert Koch Institute (RKI, 2021). Due to inaccessible data, recovered cases and active infection cases are estimated by the susceptible-exposed-infectious-removed (SEIR) model with a recovery rate of 0.0693 (Efimov and Ushirobira, 2021). The model-based results are handled by QGIS 3.8 and Python 3.7.

The WWTPs in the study area were categorized into five classes based on the maximum building capacity of WWTPs in terms of population equivalent (PE) (EKR, 2016). The inhabitant value refers to a specific biodegradable pollutant of wastewater in a sewage treatment plant. WWTPs in Classes 1–5 have the capacities of <1000 PE, 1000–5000 PE, 5001–10,000 PE, 10,001–100,000 PE and >100,000 PE, respectively.

The influences of time and space on viral pRNA concentrations were evaluated by the Kruskal–Wallis test. The Mantel test with 999 permutations based on Spearman rank correlation was used to compare the space-time matrices of infection probability and other variables of flow rates, distance to the nearest WWTPs, active infection cases, and case density in 100,000. The statistical analyses were performed using IBM SPSS Statistics 25 and R 3.6.3 with $p < 0.05$ (two-sided) as statistically significant.

## 3. Results

### 3.1. SARS-CoV-2 discharged from WWTPs

The spatiotemporal SARS-CoV-2 pRNA distribution in the WWTPs and the surface water of the Elbe watershed was simulated by the transmission model. The median results are illustrated in Fig. 2a–d. The uncertainties of the results caused by the model parameter variability are

**Table 1**
Parameters used for the dynamic QMRA model.

| Variable | Definition | Unit | Value | Reference |
|---|---|---|---|---|
| $k$ | Dose-response parameter | copies$^{-1}$ | Lognormal $(-12.24, 1.5^2)$ | (Bradburne et al., 1967; De Albuquerque et al., 2006; DeDiego et al., 2008; Hirano et al., 2001; Lunn et al., 2019; Watanabe et al., 2010; Zhang and Wang, 2020a) |
| $\alpha$ | Infection rate constant | / | Each group: 0.69–1.50 | Table S4 |
| $m$ | Water exposure dose for a swimming event | mL·person$^{-1}$·day$^{-1}$ | Children: gamma (0.81, 63) Men: gamma (0.48, 71) Women: gamma (0.52, 45) | (Schets et al., 2011) |
| $\gamma$ | First-order inactivation parameter | m$^{-1}$ | Lognormal $(-7.84, 0.45^2)$ | (Fauvel et al., 2017) |
| $r$ | Protected SARS-cov-2 RNA amount to total RNA amount ratio | % | 20.1 | (Wurtzer et al., 2021) |
| $\theta_v$ | Virus removal efficiency of WWTP | / | 3log | (Kumar et al., 2021; Yang et al., 2020) |
| $\lambda_c$ | Population connection rate to WWTP | / | 0.97 | (OECD, 2021b) |
| $\lambda_p$ | Domestic wastewater proportion | / | 0.54–0.89 | Table S5 |
| $\varphi_u$ | Toilet usage frequency constant for urine | / | Normal: 1 Lockdown: 1.13 | (Clarke and James, 2003; Gideon et al., 2019; Oakman et al., 2020; Palit et al., 2012; Rao et al., 2016), SI S1 |
| $\Phi_s$ | Toilet usage frequency constant for stool | / | Normal: 1 Lockdown: 1.96 | (Clarke and James, 2003; Gideon et al., 2019; Oakman et al., 2020; Palit et al., 2012; Rao et al., 2016), SI S1 |
| $v_u$ | Daily volume of a patient's urine | L | Gamma (5.32, 4) + 0.5 | (Rauch et al., 2003; Rose et al., 2015) |
| $n_u$ | Genome concentration of virus in a patient's urine | copies·mL$^{-1}$ | Lognormal $(5.70, 4.58^2)$ | (Jeong et al., 2020; Jones et al., 2020; Peng et al., 2020; Yang et al., 2020; Yoon et al., 2020) |
| $m_s$ | Daily mass of a patient's stool | g | Normal $(2.11, 0.25^2)$ | (Ahmed et al., 2020; Rose et al., 2015) |
| $n_s$ | Genome concentration of virus in a patient's stool | copies·g$^{-1}$ | Loguniform (6.40, 8.81) | (Wang et al., 2020; Wölfel et al., 2020; Xu et al., 2020; Zhang et al., 2021) |

shown as 95% confidence intervals (Figs. S1–3). The estimated median SARS-CoV-2 pRNA amounts in the entire wastewater system were $6.59 \times 10^9$ copies (95% CI: $3.36 \times 10^{11}$–$7.92 \times 10^7$ copies), $9.14 \times 10^8$ copies (95% CI: $4.66 \times 10^{10}$–$1.10 \times 10^7$ copies), $2.86 \times 10^8$ copies (95% CI: $1.46 \times 10^{11}$–$3.44 \times 10^7$ copies), and $1.13 \times 10^{11}$ copies (95% CI: $5.75 \times 10^{12}$–$1.35 \times 10^9$ copies) on 1st April 2020, 1st July 2020, 1st October 2020, and 1st January 2021, respectively. The states of Saxony, Thuringia, Saxony-Anhalt, and Brandenburg in the study area contributed 19.7%–55.9%, 15.2–36.4%, 18.0–40.6%, and 1.0–3.4% in the period, respectively. Furthermore, the WWTPs in Classes 2–5 treated the SARS-CoV-2 loads in wastewater daily from an average of 3, 5, 19, and 124 patients, respectively. The WWTPs in Classes 4 and 5 were responsible for approximately 95% of the SARS-CoV-2 input from the patients and output to the surface water.

In terms of virus concentrations, the virus amounts in the influent and effluent of WWTPs were transformed into concentrations by dividing the annual average daily flow of WWTP effluent. The estimated median pRNA influent concentrations were spatially distributed in the range of 0–$3.95 \times 10^1$ copies·L$^{-1}$ (95% CI: 0–$2.01 \times 10^3$ copies·L$^{-1}$), 0–$6.77 \times 10^0$ copies·L$^{-1}$ (95% CI: 0–$3.45 \times 10^2$ copies·L$^{-1}$), 0–$1.04 \times 10^1$ copies·L$^{-1}$ (95% CI: 0–$5.32 \times 10^2$ copies·L$^{-1}$) and $8.19 \times 10^0$–$3.12 \times 10^2$ copies·L$^{-1}$ (95% CI: $9.84 \times 10^{-2}$–$1.59 \times 10^4$ copies·L$^{-1}$) on 1st April 2020, 1st July 2020, 1st October 2020, and 1st January 2021, respectively. The highest daily influent concentration in the entire period ($3.65 \times 10^2$ copies·L$^{-1}$) occurred on 23rd Dec 2020. The SARS-CoV-2 concentrations in the effluent were 0.01% of the influent concentrations, and less than $3.65 \times 10^{-2}$ copies·L$^{-1}$ in the study period. Compared with the globally-reported vRNA concentrations in influent ($10^2$ to $10^6$ copies·L$^{-1}$) (Ahmed et al., 2020; Kumar et al., 2021; Randazzo et al., 2020) and effluent (0 to $10^5$ copies·L$^{-1}$) (Haramoto et al., 2020; Jones et al., 2020; Randazzo et al., 2020), the

estimated daily pRNA concentrations were relatively lower due to the low proportion of protected SARS-CoV-2 genomes in wastewater.

### 3.2. Distribution pattern of viral pRNA concentrations in the watershed

Fig. 2 illustrates the estimated median SARS-CoV-2 pRNA concentrations in the surface water of the watershed from April 2020 to January 2021. The 95% confidence interval boundaries of the results are shown in Figs. S1–3. The binned frequency distributions of the median results from April 2020 to January 2021 are shown in Fig. S4. With regard to the state-level concentration distributions, Saxony had the highest spatial-average values of $1.64 \times 10^{-4}$-$1.42 \times 10^0$ copies·L$^{-1}$ (95% CI: $1.33 \times 10^{-6}$–$1.11 \times 10^2$ copies·L$^{-1}$) during the epidemics, followed by Saxony-Anhalt ($1.45 \times 10^{-4}$–$4.21 \times 10^{-2}$ copies·L$^{-1}$; 95% CI: $1.17 \times 10^{-6}$–$3.15 \times 10^0$ copies·L$^{-1}$), Thuringia ($9.75 \times 10^{-5}$–$1.56 \times 10^{-2}$ copies·L$^{-1}$; 95% CI: $7.89 \times 10^{-7}$–$1.06 \times 10^0$ copies·L$^{-1}$), and Brandenburg ($2.09 \times 10^{-5}$–$3.01 \times 10^{-2}$ copies·L$^{-1}$; 95% CI: $1.61 \times 10^{-7}$–$2.29 \times 10^0$ copies·L$^{-1}$). Saxony also had the highest active infection cases and cases in 100,000 inhabitants among the states (Figs. S1–3), which indicates that the epidemic situation had a significant influence on the viral concentration distribution.

### 3.3. Impact of epidemic situation and virus transport on viral concentrations

The pRNA concentrations were significantly different on the temporal and spatial scales (Kruskal–Wallis test $p < 0.05$). Specifically, the temporal and spatial deviations of the estimated median results were $5.58 \times 10^{-9}$ and $7.51 \times 10^{-7}$, respectively. The spatial and temporal variation in pRNA concentrations was controlled by the epidemic situation as well as virus transport in water. The epidemic situation included regional active infection cases and active case density in the 100,000

inhabitants, while virus transport was parameterized by flow dilution and viral decay in the surface water. Compared with the active infection cases, the active case density in the 100,000 inhabitants described the regional infection rate. The flow dilution and viral decay were quantified as water flow rates and the water distance to the nearest WWTP. The correlation results examined by the Mantel test with the Spearman rank correlation ($p < 0.05$) illustrate that the epidemic situation was dominant in the temporal variation of the pRNA concentrations (Fig. 3a). Specifically, regional active infection cases and case density had larger correlation coefficients (0.74 and 0.75, respectively) than virus transport factors. This shows that the deterioration of the epidemic situation mainly contributed to the increasing pRNA concentrations on the time scale.

In contrast, virus transport significantly influenced the spatial variation in the pRNA concentrations. The flow dilution exerted a more substantial influence than the decay process. The negative correlation of the pRNA concentrations and SARS-CoV-2 transport in the surface water shows that the dilution and decay of virus in water were of importance to the reduction of viral concentrations in the surface water. The dilution performance could be parameterized as a dilution factor, which is a ratio of the surface water to wastewater flow from the WWTPs. A factor of >40 is suggested by engineering practice to prevent the infection risk of viruses (Kumar et al., 2021). The average dilution factor near the WWTPs was 2584.9 in the studied period. A total of 43.2%–71.1% of the

dilution factors in the Elbe watershed were >40 (Fig. 3b). Additionally, due to viral decay, the pRNA spatial-average amount in the surface water decreased from $1.17 \times 10^8$ copies to $1.31 \times 10^{-2}$ copies with increasing transmission distance (from 0 m to 326,000 m) (Fig. 3c). There were some sudden increases in the distance-dependent pRNA amount reduction, which might be caused by virus accumulation from the residual upstream.

The analysis suggests that the case density and the flow rate in the surface water were two fundamental variables and affected the spatial and temporal variation of pRNA concentrations in the surface water. The water near the WWTPs had higher pRNA concentrations.

### 3.4. Infection probability in different scenarios and population groups

The infection probabilities of SARS-CoV-2 from surface water ingestion during swimming were separately estimated under the scenarios of normal and increasing toilet usage frequencies, the age groups (5–14, 15–34, 5–59, and 60–79 years old), and the gender groups. The toilet usage frequency variation was caused by the patients' psychological stress during the lockdown, which resulted in the change in viral concentrations in wastewater and surface water.

Fig. 4a illustrates the estimated probability of infection with SARS-CoV-2 for different scenarios and population groups. The difference in infection probability was apparent in toilet usage
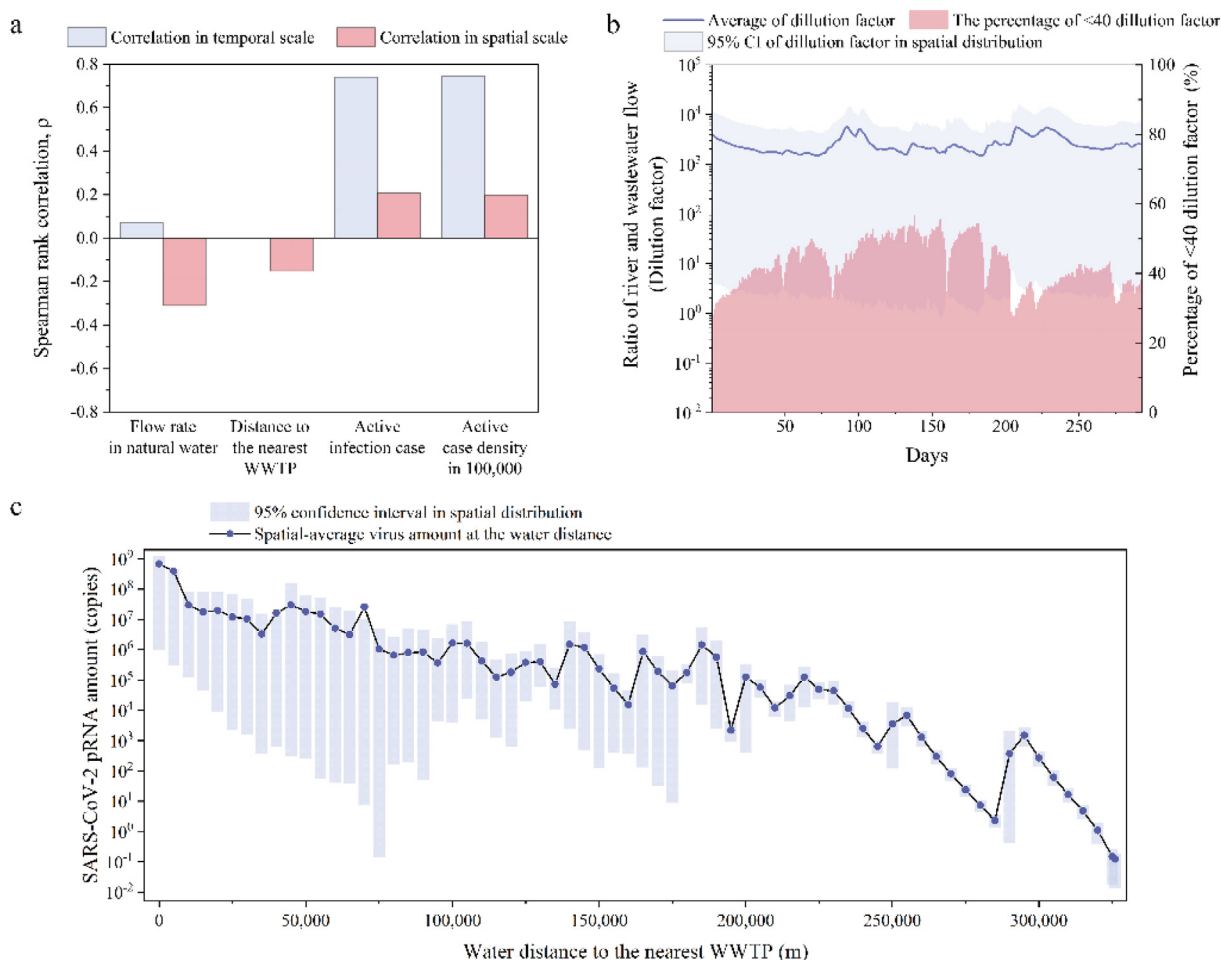


**Fig. 3.** a). Spearman rank correlation between the SARS-CoV-2 pRNA concentrations in the surface water and flow rates of surface water, distances to the nearest WWTP, active infection cases as well as infection cases in 100,000 population via the Mantel test. b) Dilution factors monitored at the water point near the WWTPs with 95% confidence interval in spatial distribution, corresponding to the left y-axis, and percentages of <40 dilution factors, corresponding to the right y-axis. Day zero corresponds to 25th March 2020. c) The decay of SARS-CoV-2 pRNA amount in the surface water corresponding to the water distance away from the nearest WWTPs with a 95% confidence interval in spatial distribution. The values were the median of the Monte-Carlo uncertainty results.
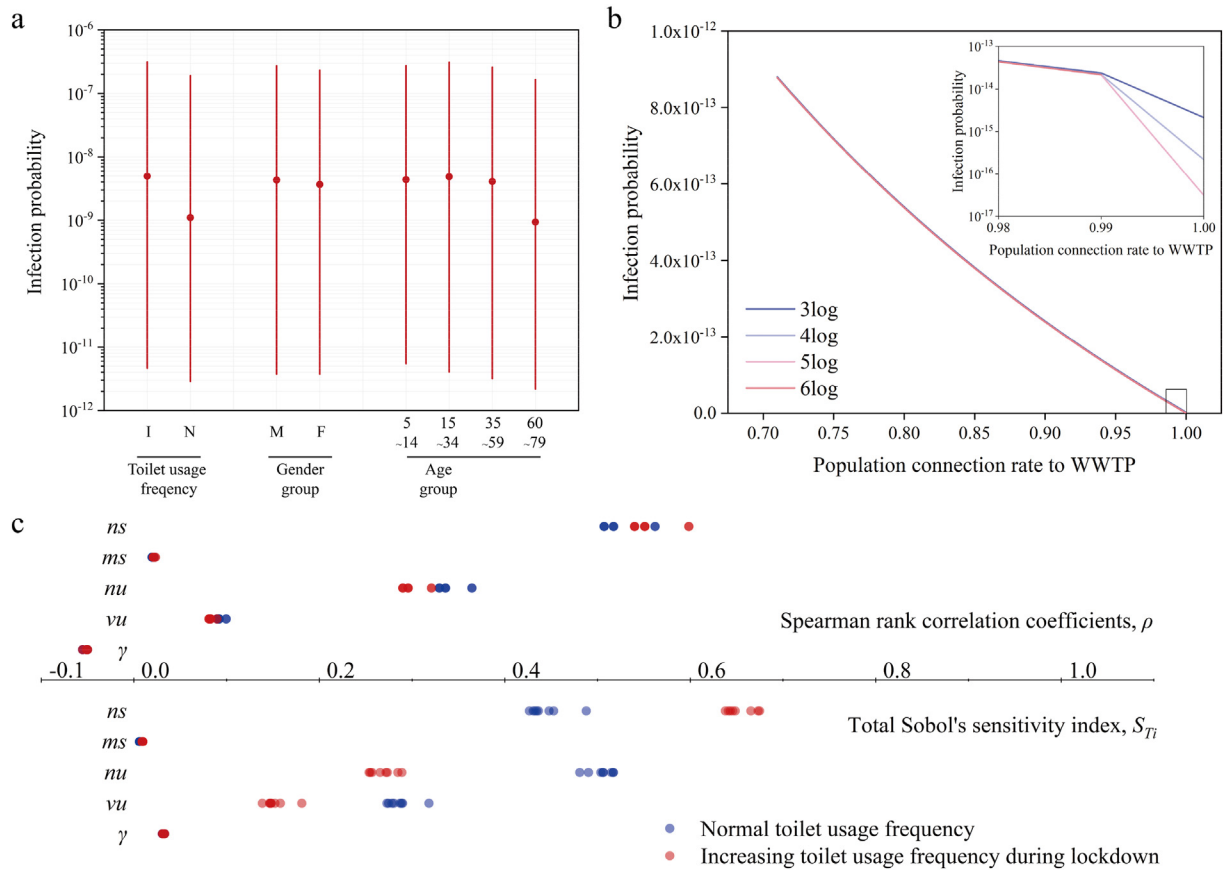
**Fig. 4.** a). The median infection probabilities in the scenarios of toilet usage frequency as well as population groups in different genders and ages. The red dot for each scenario or population group represented the average result among other scenarios and population groups with estimated median values. The red lines were a 95% confidence interval (CI) controlled by distributed parameters. b) The change of infection probability caused by the virus removal efficiencies of WWTPs and population connection rates to WWTPs. c) The Spearman rank correlation coefficient and the total Sobol's sensitivity index between seven model parameters and the infection probability in the scenarios of toilet usage frequency as well as the groups of gender and age.

frequency. Specifically, the potentially increasing toilet usage frequency during the lockdown increased the infection probability on average from $1.10 \times 10^{-9}$ to $4.94 \times 10^{-9}$.

Regarding the population groups, men had a comparable infection probability with a spatiotemporal median of $4.30 \times 10^{-9}$ (95% CI: $3.74 \times 10^{-12}$–$2.73 \times 10^{-7}$) compared with the infection probability of women ($3.66 \times 10^{-9}$, 95% CI: $3.74 \times 10^{-12}$–$2.32 \times 10^{-7}$). This result was different from the statistics reported by Robert Koch-Institut (RKI, 2021) that the female adults (812,739) had more infection cases than men (764,026) in Germany. The difference might be caused by the uncertainty of the exposure water dose for men and women. Additionally, the population aged 15–34 years had the highest probability of infection ($4.86 \times 10^{-9}$; 95% CI: $4.05 \times 10^{-12}$–$3.09 \times 10^{-7}$) among the age groups. The results were consistent with the report that the population aged 15–34 years was the most infected population in Germany (RKI, 2021).

It should be noted that all the spatiotemporal distributed infection probabilities in the study period were significantly lower than the daily-transformed reference risk levels of $10^{-4}$ and $10^{-5}$ suggested by the US EPA (Gholipour et al., 2021) and WHO (Mara et al., 2007) respectively. This suggests that waterborne transmission was a less important transmission route for SARS-CoV-2 than air transmission.

### 3.5. Influencing factor of infection probability

As excretions were the potential source of SARS-CoV-2 loading to wastewater and surface water, WWTPs played a crucial role in controlling the transmission of SARS-CoV-2 pRNA. The main associated technical parameters were virus removal efficiency $\theta_v$ and population

connection rates to WWTPs, $\lambda_c$. Fig. 4b illustrates the impact of these two parameters on the spatiotemporally average infection probabilities along the Elbe main channel. $\theta_v$ was selected in the range of 3log–6log based on the references (Bhowmick et al., 2020; Kumar et al., 2021; Zhang et al., 2016). $\lambda_c$ was in the range of 0.71–1 based on the percentage of the resident population connected to urban wastewater collecting systems in 2016–2018 in 35 countries (OECD, 2021b) (Table S9). Interestingly, the increase in $\lambda_c$ reduced the infection probabilities of SARS-CoV-2 by two orders of magnitude from an average of $8.78 \times 10^{-13}$ to $5.99 \times 10^{-16}$. The changes in $\theta_v$ had no apparent impacts on the infection probability until the 100% resident population connected to WWTPs.

Fig. 4c shows the sensitivity analysis of the infection probability to seven distributed-based parameters ($k$, $m$, $\gamma$, $v_u$, $n_u$, $m_s$, and $n_s$) in different scenarios and groups. The global Sobol's sensitivity index ($S_{Ti}$) and the Spearman rank correlation coefficients ($\rho$) were employed. The dose-response parameter ($k$), the water exposure dose ($m$), and the genome concentration of patients' stool ($n_s$) were dominant factors that affected the infection probability. The former two parameters are directly related to the dose-response model. The sensitivity result of $n_s$ was consistent with prior reviews that patient excretions, especially faeces, were the main sources of SARS-CoV-2 transmission in wastewater (Bhowmick et al., 2020; Jones et al., 2020). The distributed variations of these parameters were mainly responsible for the uncertainties of the model estimation. In contrast, the first-order inactivation parameter ($\gamma$), the daily mass of a patient's stool ($m_s$), and the genome concentration of virus in a patient's urine ($v_u$) weakly affected the infection probability in surface water.

The toilet usage frequency scenario showed significant impacts on the sensitivity results of the sewage parameters ($v_u$, $n_u$, $m_s$, and $n_s$) (Mann–Whitney $U$ test $p < 0.05$), as shown in Table S10. Specifically, the increasing toilet usage frequency resulted in a 50% increase in $S_{Ti}$ (6% for $\rho$) of $m_s$, and $n_s$, but a 50% decrease in $S_{Ti}$ (10% for $\rho$) of $m_u$, and $n_u$. However, the gender and age groups exerted a limited impact on the sensitivity variation.

## 4. Discussion

The results of the study reflected that the WWTP was an important sector between domestic wastewater and surface water. On the one hand, most of the SARS-CoV-2 discharged into the surface water came from WWTPs, especially WWTPs in urban areas. Over 90% of SARS-CoV-2 in virus-contaminated domestic wastewater was discharged from the WWTPs with a maximum capacity of >10,000 population equivalents. These WWTPs were located around urban cities, indicating that urban areas were the major contributors to virus-contaminated wastewater. On the other hand, the SARS-CoV-2 concentration in the wastewater was expected to be mostly removed in WWTPs. However, the removal efficiency of SARS-CoV-2 in the wastewater treatment of WWTPs ranges widely and is still largely unexplored specifically for SARS-CoV-2. Several studies and reviews have estimated or investigated the removal efficiencies of SARS-CoV-2 RNA for various conventional activated sludge (CAS) processes (Abu Ali et al., 2021; Bogler et al., 2020; Kumar et al., 2021). The results show that the removal efficiency of SARS-CoV-2 vRNA in WWTPs would be in the range of between 2log and 6log. It seems that the infectious particles were less stable than the total RNA in the water (Sala-Comorera et al., 2021), which suggests that the removal efficiency of pRNA should be higher. For advanced treatment processes, chlorination, ozone, and UV irradiation could significantly inactivate SARS-CoV-2 (Heilingloh et al., 2020; Zhang et al., 2020). However, no WWTPs in the study area have chlorination, ozone, and UV treatments, which might be a concern regarding the potential spread of SARS-CoV-2. Combined with the abovementioned removal efficiencies and the wastewater treatment process data, the removal efficiency of 3log was selected to simulate SARS-CoV-2 RNA reduction in WWTPs.

To confirm the impact of the removal efficiency in WWTPs on the infection risk of SARS-CoV-2, a removal efficiency between 3–6log was analysed. The result shows that the increase in removal efficiencies for wastewater treatment processes had a limited impact on the infection probability from surface water ingestion. This suggests that the improvement of the population connection rate to WWTPs took priority over the enhancement of the SARS-CoV-2 treatment technique, especially in developing countries with low population connection rates to WWTPs, although a tertiary treatment is an additional important barrier (Abu Ali et al., 2021).

Furthermore, the distribution of SARS-CoV-2 pRNA in the surface water was related not only to the WWTPs but also to other factors, such as the dilution of viruses by surface water. The dilution process was driven by the dynamics of water flows, which had seasonal variations (Kumar et al., 2021). This resulted in seasonal changes in pRNA concentrations in the watershed (Fig. 2). The dilution factors were higher in June–July 2020 (average 2800.0) and October–November 2020 (average 3726.4) (Fig. 3b). Compared with the temporal changes in water flows, the spatial variation in the flow in the watershed was more important to the distribution of viral concentrations in the surface water according to the correlation result.

Regarding the infection probability of SARS-CoV-2 from surface water ingestion, it is worth noting that the lockdown policy in the study area could not eliminate the probability of surface water ingestion during the epidemics. The lockdown measure mainly prohibits gatherings, but individual outdoor activities are allowed in Germany (Anke et al., 2021). A survey shows that children's and adolescents' activity time of nonorganized sports increased by 100%–400% after the COVID-19

lockdown in Germany (Schmidt et al., 2020). The increase in outdoor activities might increase the probability of surface water ingestion during swimming activities.

The infection probabilities of SARS-CoV-2 from surface water ingestion were estimated in different scenarios and population groups. Interestingly, the variation in toilet usage frequencies caused by the patients' psychological changes during the lockdown had an impact on the infection probabilities. The lockdown intervention physically distances social contact and restricts movement, which mainly reduces the risk of virus transmission through infected people and aerosols. However, it might show a distinctive effect on the infection probability of SARS-CoV-2 from surface water ingestion, as the source of the virus comes from excrements in the toilet. As shown in Supplementary material S1, the work-at-home population during lockdown relieves psychosocial stress and physical stress, increasing urination and defaecation frequency. The lockdown might slightly amplify the probability in the surface water when the lockdown starts, but the lockdown policy is still the effective approach to slow COVID-19 transmission (WHO, 2020).

The model-based results presented in this work remained uncertain, although we highly improved the reliability of the results by using pRNA instead of vRNA in the calculation of viral concentrations in the surface water and analyzing the uncertainty and sensitivity of the model parameters. By using the pRNA/vRNA ratio as a model parameter, the model was able to estimate the more infectious SARS-CoV-2 concentrations in surface water rather than the total SARS-CoV-2 RNA concentrations, including the noninfectious particles (Dada and Gyawali, 2021; Yang et al., 2020; Zaneti et al., 2021). However, pRNA includes the protected genomes within infectious particles and noninfectious particles in a ribonucleoprotein complex (Wurtzer et al., 2021). Therefore, there might be a slight overestimation in the results. In addition, the model-based results were affected by the model parameters. The large 95% confidence intervals of the results indicate that the model parameter variations had a significant influence on the simulation results of the viral concentration distribution and the infection probability. Except for the parameters considered in the study, the model was also inherently limited by other uncertainties from the unknown information, such as the lack of inactivation or the reduction of viral pRNA in the sewage system and the detailed physical-chemical properties of the surface water. Specifically, the parameters of pH, temperature, suspended solids, and pharmaceuticals in water could influence SARS-CoV-2 concentrations (de Oliveira et al., 2021; Dehbandi and Zazouli, 2020; Geller et al., 2012; Kumar et al., 2019). The model can be further improved if SARS-CoV-2 is more deeply investigated and comprehensively understood.

## 5. Conclusion

This study provides an approach considering the transmission of SARS-CoV-2 protected RNA genomes (pRNA) from infected individuals and a wastewater collecting system to surface water. The viral pRNA concentrations increased with the increase in active infection cases. The water flow and viral inactivation process considerably reduced the virus concentrations. The infection risk analysis shows that the population aged 15–34 years has the highest infection probability when exposed to aqueous environments. The increase in toilet usage frequency induced by the work-at-home population during lockdown could increase the infection probability. However, the low pRNA concentrations and infection probability reflect that the waterways were unlikely to be a significant transmission route for SARS-CoV-2. The data provided herein suggest that improving the population connection rate to WWTPs could be more effective in alleviating the infection probability from virus-contaminated surface water.

## CRediT authorship contribution statement

**Zhenyu Wang**: Conceptualization, Methodology, Software, Formal analysis, Investigation, Data Curation, Writing - Original Draft,

Visualization **Wenyu Yang**: Conceptualization, Methodology, Investigation, Data Curation, Writing - Review & Editing **Hua Pei**: Conceptualization, Writing - Review & Editing, Supervision **Jin Zhang**: Supervision **Peter Krebs**: Supervision.

## Declaration of competing interest

The authors declare that they have no known competing financial interests or personal relationships that could have appeared to influence the work reported in this paper.

## Acknowledgments

## Appendix A. Supplementary data

Supplementary data to this article can be found online at https://doi.org/10.1016/j.scitotenv.2021.150888.

## References

Abu Ali, H., Yaniv, K., Bar-Zeev, E., Chaudhury, S., Shagan, M., Lakkakula, S., et al., 2021. Tracking SARS-CoV-2 RNA through the wastewater treatment process. ACS ES&T Water 1, 1161–1167. https://doi.org/10.1021/acsestwater.0c00216.

Ahmed, W., Angel, N., Edson, J., Bibby, K., Bivins, A., O'Brien, J.W., et al., 2020. First confirmed detection of SARS-CoV-2 in untreated wastewater in Australia: a proof of concept for the wastewater surveillance of COVID-19 in the community. Sci. Total Environ. 728. https://doi.org/10.1016/j.scitotenv.2020.138764.

Ahmed, W., Bibby, K., D'Aoust, P., Delatolla, R., Gerba, C., Haas, C., et al., 2021. Differentiating between the possibility and probability of SARS-CoV-2 transmission associated with wastewater: empirical evidence is needed to substantiate risk. FEMS Microbes 2. https://doi.org/10.1093/femsmc/xtab007.

Anke, J., Francke, A., Schaefer, L.-M., Petzoldt, T., 2021. Impact of SARS-CoV-2 on the mobility behaviour in Germany. Eur. Transp. Res. Rev. 13, 10. https://doi.org/10.1186/s12544-021-00469-3.

Asadi, S., Bouvier, N., Wexler, A.S., Ristenpart, W.D., 2020. The coronavirus pandemic and aerosols: does COVID-19 transmit via expiratory particles? Aerosol Sci. Technol. 54, 635–638. https://doi.org/10.1080/02786826.2020.1749229.

Bhowmick, G.D., Dhar, D., Nath, D., Ghangrekar, M.M., Banerjee, R., Das, S., et al., 2020. Coronavirus disease 2019 (COVID-19) outbreak: some serious consequences with urban and rural water cycle. npj clean Water 3, 32. https://doi.org/10.1038/s41545-020-0079-1.

Bivins, A.W., Sumner, T., Kumpel, E., Howard, G., Cumming, O., Ross, I., et al., 2017. Estimating infection risks and the global burden of diarrheal disease attributable to intermittent water supply using QMRA. Environmental Science & Technology. 51, 7542–7551. https://doi.org/10.1021/acs.est.7b01014.

Bogler, A., Packman, A., Furman, A., Gross, A., Kushmaro, A., Ronen, A., et al., 2020. Rethinking wastewater risks and monitoring in light of the COVID-19 pandemic. Nature Sustainability 3, 981–990. https://doi.org/10.1038/s41893-020-00605-2.

Bradburne, A.F., Bynoe, M.L., Tyrrell, D.A., 1967. Effects of a "new" human respiratory virus in volunteers. Br. Med. J. 3, 767–769. https://doi.org/10.1136/bmj.3.5568.767.

Chan, J.F.-W., Yuan, S., Kok, K.-H., To, K.K.-W., Chu, H., Yang, J., et al., 2020. A familial cluster of pneumonia associated with the 2019 novel coronavirus indicating person-to-person transmission: a study of a family cluster. Lancet 395, 514–523. https://doi.org/10.1016/S0140-6736(20)30154-9.

Chia, P.Y., Coleman, K.K., Tan, Y.K., Ong, S.W.X., Gum, M., Lau, S.K., et al., 2020. Detection of air and surface contamination by SARS-CoV-2 in hospital rooms of infected patients. Nat. Commun. 11, 2800. https://doi.org/10.1038/s41467-020-16670-2.

Clarke, J.N., James, S., 2003. The radicalized self: the impact on the self of the contested nature of the diagnosis of chronic fatigue syndrome. Soc. Sci. Med. 57, 1387–1395. https://doi.org/10.1016/S0277-9536(02)00515-4.

Dada, A.C., Gyawali, P., 2021. Quantitative microbial risk assessment (QMRA) of occupational exposure to SARS-CoV-2 in wastewater treatment plants. Sci. Total Environ. 763. https://doi.org/10.1016/j.scitotenv.2020.142989.

De Albuquerque, N., Baig, E., Ma, X., Zhang, J., He, W., Rowe, A., et al., 2006. MurineHepatitis virus strain 1 produces a clinically relevant model of severe acute respiratory syndrome in A/J mice. J. Virol. 80, 10382–10394. https://doi.org/10.1128/jvi.00747-06.

de Oliveira, L.C., Torres-Franco, A.F., Lopes, B.C., Santos, B.S.Á.d.S., Costa, E.A., Costa, M.S., et al., 2021. Viability of SARS-CoV-2 in river water and wastewater at different temperatures and solids content. Water Res. 195. https://doi.org/10.1016/j.watres.2021.117002.

DeDiego, M.L., Pewe, L., Alvarez, E., Rejas, M.T., Perlman, S., Enjuanes, L., 2008. Pathogenicity of severe acute respiratory coronavirus deletion mutants in hACE-2 transgenic mice. Virology 376, 379–389. https://doi.org/10.1016/j.virol.2008.03.005.

Dehbandi, R., Zazouli, M.A., 2020. Stability of SARS-CoV-2 in different environmental conditions. The Lancet Microbe. 1, e145. https://doi.org/10.1016/S2666-5247(20)30093-8.

Efimov, D., Ushirobira, R., 2021. On an interval prediction of COVID-19 development based on a SEIR epidemic model. Annu. Rev. Control. https://doi.org/10.1016/j.arcontrol.2021.01.006.

EKR, 2016. Europäische Kommunalabwasser-Richtlinie in Deutschland. https://kommunales-abwasser.de/. (Accessed 23 February 2021).

Fauvel, B., Gantzer, C., Cauchie, H.-M., Ogorzaly, L., 2017. In situ dynamics of F-specific RNA bacteriophages in a Small River: new way to assess viral propagation in water quality studies. Food and Environmental Virology. 9, 89–102. https://doi.org/10.1007/s12560-016-9266-0.

Geller, C., Varbanov, M., Duval, R.E., 2012. Human coronaviruses: insights into environmental resistance and its influence on the development of new antiseptic strategies. Viruses 4, 3044–3068. https://doi.org/10.3390/v4113044.

Gholipour, S., Mohammadi, F., Nikaeen, M., Shamsizadeh, Z., Khazeni, A., Sahbaei, Z., et al., 2021. COVID-19 infection risk from exposure to aerosols of wastewater treatment plants. Chemosphere 273. https://doi.org/10.1016/j.chemosphere.2021.129701.

Gideon, A., Sauter, C., Fieres, J., Berger, T., Renner, B., Wirtz, P.H., 2019. Kinetics and interrelations of the renin aldosterone response to acute psychosocial stress: a neglected stress system. J. Clin. Endocrinol. Metab. 105, e762–e773. https://doi.org/10.1210/clinem/dgz190.

Gormley, M., Aspray, T.J., Kelly, D.A., 2020. COVID-19: mitigating transmission via wastewater plumbing systems. Lancet Glob. Health 8, e643.

Guan, W.-j., Ni, Z.-y., Hu, Y., Liang, W.-h., Ou, C.-q., He, J.-x., et al., 2020. Clinical characteristics of coronavirus disease 2019 in China. N. Engl. J. Med. 382, 1708–1720. https://doi.org/10.1056/NEJMoa2002032.

Guerrero-Latorre, L., Ballesteros, I., Villacrés-Granda, I., Granda, M.G., Freire-Paspuel, B., Ríos-Touma, B., 2020. SARS-CoV-2 in river water: implications in low sanitation countries. Sci. Total Environ. 743. https://doi.org/10.1016/j.scitotenv.2020.140832.

Haas, C.N., Rose, J.B., Gerba, C.P., 2014. Quantitative microbial risk assessment. John Wiley & Sons.

Haramoto, E., Malla, B., Thakali, O., Kitajima, M., 2020. First environmental surveillance for the presence of SARS-CoV-2 RNA in wastewater and river water in Japan. Sci. Total Environ. 737. https://doi.org/10.1016/j.scitotenv.2020.140405.

Heilingloh, C.S., Aufderhorst, U.W., Schipper, L., Dittmer, U., Witzke, O., Yang, D., et al., 2020. Susceptibility of SARS-CoV-2 to UV irradiation. Am. J. Infect. Control 48, 1273–1275. https://doi.org/10.1016/j.ajic.2020.07.031.

Hirano, N., Haga, S., Sada, Y., Tohyama, K., 2001. Susceptibility of rats of different ages to inoculation with swine haemagglutinating encephalomyelitis virus (a Coronavirus) by various routes. J. Comp. Pathol. 125, 8–14. https://doi.org/10.1053/jcpa.2001.0471.

Jeong, H.W., Kim, S.-M., Kim, H.-S., Kim, Y.-I., Kim, J.H., Cho, J.Y., et al., 2020. Viable SARS-CoV-2 in various specimens from COVID-19 patients. Clin. Microbiol. Infect. 26, 1520–1524. https://doi.org/10.1016/j.cmi.2020.07.020.

Jones, D.L., Baluja, M.Q., Graham, D.W., Corbishley, A., McDonald, J.E., Malham, S.K., et al., 2020. Shedding of SARS-CoV-2 in feces and urine and its potential role in person-to-person transmission and the environment-based spread of COVID-19. Sci. Total Environ. 749. https://doi.org/10.1016/j.scitotenv.2020.141364.

Kissler, S.M., Tedijanto, C., Goldstein, E., Grad, Y.H., Lipsitch, M., 2020. Projecting the transmission dynamics of SARS-CoV-2 through the postpandemic period. Science 368, 860. https://doi.org/10.1126/science.abb5793.

Kraemer, M.U.G., Yang, C.-H., Gutierrez, B., Wu, C.-H., Klein, B., Pigott, D.M., et al., 2020. The effect of human mobility and control measures on the COVID-19 epidemic in China. Science 368, 493. https://doi.org/10.1126/science.abb4218.

Kumar, M., Ram, B., Honda, R., Poopipattana, C., Canh, V.D., Chaminda, T., et al., 2019. Concurrence of antibiotic resistant bacteria (ARB), viruses, pharmaceuticals and personal care products (PPCPs) in ambient waters of Guwahati, India: urban vulnerability and resilience perspective. Sci. Total Environ. 693. https://doi.org/10.1016/j.scitotenv.2019.133640.

Kumar, M., Alamin, M., Kuroda, K., Dhangar, K., Hata, A., Yamaguchi, H., et al., 2021. Potential discharge, attenuation and exposure risk of SARS-CoV-2 in natural water bodies receiving treated wastewater. npj clean Water 4, 8. https://doi.org/10.1038/s41545-021-00098-2.

Lunn, T.J., Restif, O., Peel, A.J., Munster, V.J., Ed, Wit, Sokolow, S., et al., 2019. Dose-response and transmission: the nexus between reservoir hosts, environment and recipient hosts. 374. https://doi.org/10.1098/rstb.2019.0016.

Mara, D., Sleigh, P., Blumenthal, U., Carr, R., 2007. Health risks in wastewater irrigation: comparing estimates from quantitative microbial risk analyses and epidemiological studies. J. Water Health 5, 39–50.

Mawani, M., Li, C., 2020. Coronavirus disease (COVID-19); lessons learnt from international response and advice to the Georgia government. The Innovation 1. https://doi.org/10.1016/j.xinn.2020.100025.

McKinney, K.R., Gong, Y.Y., Lewis, T.G., 2006. Environmental transmission of SARS at Amoy Gardens. J. Environ. Health 68, 26–30.

Moazeni, M., Nikaeen, M., Hadi, M., Moghim, S., Mouhebat, L., Hatamzadeh, M., et al., 2017. Estimation of health risks caused by exposure to enteroviruses from agricultural application of wastewater effluents. Water Res. 125, 104–113. https://doi.org/10.1016/j.watres.2017.08.028.

Mohapatra, S., Menon, N.G., Mohapatra, G., Pisharody, L., Pattnaik, A., Menon, N.G., et al., 2021. The novel SARS-CoV-2 pandemic: possible environmental transmission, detection, persistence and fate during wastewater and water treatment. Sci. Total Environ. 765. https://doi.org/10.1016/j.scitotenv.2020.142746.

Oakman, J., Kinsman, N., Stuckey, R., Graham, M., Weale, V., 2020. A rapid review of mental and physical health effects of working at home: how do we optimise health? BMC Public Health 20, 1825. https://doi.org/10.1186/s12889-020-09875-z.

OECD, 2021a. Real GDP forecast by Organisation for Economic Co-operation and Development. https://data.oecd.org/gdp/real-gdp-forecast.htm. (Accessed 27 February 2021).

OECD, 2021b. Wastewater treatment recorded by OECD.Stat. https://stats.oecd.org/Index.aspx?DataSetCode=WATER_TREAT. (Accessed 1 March 2021).

Palit, S., Lunniss, P.J., Scott, S.M., 2012. The physiology of human defecation. Dig. Dis. Sci. 57, 1445–1464. https://doi.org/10.1007/s10620-012-2071-1.

Pan, Y., Zhang, D., Yang, P., Poon, L.L.M., Wang, Q., 2020. Viral load of SARS-CoV-2 in clinical samples. Lancet Infect. Dis. 20, 411–412. https://doi.org/10.1016/S1473-3099(20)30113-4.

Paul, D., Kolar, P., Hall, S.G., 2021. A review of the impact of environmental factors on the fate and transport of coronaviruses in aqueous environments. npj clean Water 4, 7. https://doi.org/10.1038/s41545-020-00096-w.

Peng, L., Liu, J., Xu, W., Luo, Q., Chen, D., Lei, Z., et al., 2020. SARS-CoV-2 can be detected in urine, blood, anal swabs, and oropharyngeal swabs specimens. J. Med. Virol. 92, 1676–1680.

Penn, R., Ward, B.J., Strande, L., Maurer, M., 2018. Review of synthetic human faeces and faecal sludge for sanitation and wastewater research. Water Res. 132, 222–240.

Randazzo, W., Truchado, P., Cuevas-Ferrando, E., Simón, P., Allende, A., Sánchez, G., 2020. SARS-CoV-2 RNA in wastewater anticipated COVID-19 occurrence in a low prevalence area. Water Res. 181. https://doi.org/10.1016/j.watres.2020.115942.

Rao, S.S.C., Bharucha, A.E., Chiarioni, G., Felt-Bersma, R., Knowles, C., Malcolm, A., et al., 2016. Anorectal disorders. Gastroenterology 150, 1430–1442.e4. https://doi.org/10.1053/j.gastro.2016.02.009.

Rauch, W., Brockmann, D., Peters, I., Larsen, T.A., Gujer, W., 2003. Combining urine separation with waste design: an analysis using a stochastic model for urine production. Water Res. 37, 681–689. https://doi.org/10.1016/S0043-1354(02)00364-0.

RKI, 2021. COVID-19 (Coronavirus SARS-CoV-2). https://www.rki.de/DE/Content/InfAZ/N/Neuartiges_Coronavirus/nCoV_node.html. (Accessed 15 January 2021).

Rose, C., Parker, A., Jefferson, B., Cartmell, E., 2015. The characterization of feces and urine: a review of the literature to inform advanced treatment technology. Crit. Rev. Environ. Sci. Technol. 45, 1827–1879. https://doi.org/10.1080/10643389.2014.1000761.

Sala-Comorera, L., Reynolds, L.J., Martin, N.A., O'Sullivan, J.J., Meijer, W.G., Fletcher, N.F., 2021. Decay of infectious SARS-CoV-2 and surrogates in aquatic environments. Water Res. 201. https://doi.org/10.1016/j.watres.2021.117090.

Schets, F.M., Schijven, J.F., de Roda Husman, A.M., 2011. Exposure assessment for swimmers in bathing waters and swimming pools. Water Res. 45, 2392–2400. https://doi.org/10.1016/j.watres.2011.01.025.

Schmidt, S.C.E., Anedda, B., Burchartz, A., Eichsteller, A., Kolb, S., Nigg, C., et al., 2020. Physical activity and screen time of children and adolescents before and during the COVID-19 lockdown in Germany: a natural experiment. Sci. Rep. 10, 21780. https://doi.org/10.1038/s41598-020-78438-4.

Sobol, I.M., 2001. Global sensitivity indices for nonlinear mathematical models and their Monte Carlo estimates. Math. Comput. Simul. 55, 271–280.

Vezzaro, L., Mikkelsen, P.S., 2012. Application of global sensitivity analysis and uncertainty quantification in dynamic modelling of micropollutants in stormwater runoff. Environ. Model Softw. 27–28, 40–51. https://doi.org/10.1016/j.envsoft.2011.09.012.

Wang, W., Xu, Y., Gao, R., Lu, R., Han, K., Wu, G., et al., 2020. Detection of SARS-CoV-2 in different types of clinical specimens. JAMA 323, 1843–1844. https://doi.org/10.1001/jama.2020.3786.

Watanabe, T., Bartrand, T.A., Weir, M.H., Omura, T., Haas, C.N., 2010. Development of a dose-response model for SARS coronavirus. Risk Anal. 30, 1129–1138. https://doi.org/10.1111/j.1539-6924.2010.01427.x.

WHO, 2020. Coronavirus disease (COVID-19): Herd immunity, lockdowns and COVID-19. https://www.who.int/news-room/q-a-detail/herd-immunity-lockdowns-and-covid-19. (Accessed 17 March 2021).

WHO, 2021. WHO Coronavirus Disease (COVID-19) Dashboard. https://covid19.who.int/table. (Accessed 27 February 2021).

Wölfel, R., Corman, V.M., Guggemos, W., Seilmaier, M., Zange, S., Müller, M.A., et al., 2020. Virological assessment of hospitalized patients with COVID-2019. Nature 581, 465–469.

Wurtzer, S., Waldman, P., Ferrier-Rembert, A., Frenois-Veyrat, G., Mouchel, J.M., Boni, M., et al., 2021. Several forms of SARS-CoV-2 RNA can be detected in wastewaters: implication for wastewater-based epidemiology and risk assessment. Water Res. 198. https://doi.org/10.1016/j.watres.2021.117183.

Xu, Y., Li, X., Zhu, B., Liang, H., Fang, C., Gong, Y., et al., 2020. Characteristics of pediatric SARS-CoV-2 infection and potential evidence for persistent fecal viral shedding. Nat. Med. 26, 502–505. https://doi.org/10.1038/s41591-020-0817-4.

Yang, B., Li, W., Wang, J., Tian, Z., Cheng, X., Zhang, Y., et al., 2020. Estimation of the potential spread risk of COVID-19: occurrence assessment along the Yangtze, Han, and Fu River basins in Hubei, China. 746. https://doi.org/10.1016/j.scitotenv.2020.141353.

Yoon, J.G., Yoon, J., Song, J.Y., Yoon, S.-Y., Lim, C.S., Seong, H., et al., 2020. Clinical significance of a high SARS-CoV-2 viral load in the saliva. J. Korean Med. Sci. 35.

Yu, I.T.-S., Qiu, H., Tse, L.A., Wong, T.W., 2014. Severe acute respiratory syndrome beyond Amoy gardens: completing the incomplete legacy. Clin. Infect. Dis. 58, 683–686.

Zaneti, R.N., Girardi, V., Spilki, F.R., Mena, K., Westphalen, A.P.C., da Costa Colares, E.R., et al., 2021. Quantitative microbial risk assessment of SARS-CoV-2 for workers in wastewater treatment plants. Sci. Total Environ. 754. https://doi.org/10.1016/j.scitotenv.2020.142163.

Zhang, X., Wang, J., 2020. Deducing the dose-response relation for coronaviruses from COVID-19, SARS and MERS meta-analysis results. https://doi.org/10.1101/2020.06.26.20140624.

Zhang, X., Wang, J., 2020b. Dose-response relation deduced for coronaviruses from COVID-19, SARS and MERS meta-analysis results and its application for infection risk assessment of aerosol transmission. Clin. Infect. Dis. https://doi.org/10.1093/cid/ciaa1675.

Zhang, C.-M., Xu, L.-M., Xu, P.-C., Wang, X.C., 2016. Elimination of viruses from domestic wastewater: requirements and technologies. World J. Microbiol. Biotechnol. 32, 69. https://doi.org/10.1007/s11274-016-2018-3.

Zhang, D., Ling, H., Huang, X., Li, J., Li, W., Yi, C., et al., 2020. Potential spreading risks and disinfection challenges of medical wastewater by the presence of severe acute respiratory syndrome coronavirus 2 (SARS-CoV-2) viral RNA in septic tanks of Fangcang Hospital. Sci. Total Environ. 741. https://doi.org/10.1016/j.scitotenv.2020.140445.

Zhang, N., Gong, Y., Meng, F., Shi, Y., Wang, J., Mao, P., et al., 2021. Comparative study on virus shedding patterns in nasopharyngeal and fecal specimens of COVID-19 patients. Sci. China Life Sci. 64, 486–488. https://doi.org/10.1007/s11427-020-1783-9.